

Stable Fractional Vortices in the Cyclic States of Bose-Einstein Condensates

J. A. M. Huhtamäki,^{1,2} T. P. Simula,¹ M. Kobayashi,³ and K. Machida¹

¹*Department of Physics, Okayama University, Okayama 700-8530, Japan*

²*Department of Applied Physics, Helsinki University of Technology, P.O. Box 5100, 02015 TKK, Finland and*

³*Department of Physics, University of Tokyo, Hongo 7-3-11, Bunkyo-ku, Tokyo 113-0033, Japan*

We propose methods to create fractional vortices in the cyclic state of an $F = 2$ spinor Bose-Einstein condensate by manipulating its internal spin structure using pulsed microwave and laser fields. The stability of such vortices is studied as a function of the rotation frequency of the confining harmonic trap both in pancake and cigar shaped condensates. We find a range of parameters for which the so-called $1/3$ -vortex state is energetically favorable. Such fractional vortices could be created in condensates of ^{87}Rb atoms using current experimental techniques facilitating probing of topological defects with non-Abelian statistics.

The peculiar nature of quantum fluids stands out remarkably when observing their rotational characteristics. Rigid-body rotation is forbidden for a superfluid due to the constraint that its velocity field is bound to be irrotational. Instead they may acquire angular momentum by hosting a number of quantized vortex lines [1]. The superfluid state is characterized in terms of an order parameter which in general is a multicomponent complex function. In the single-component (scalar) case, the quantized vortex lines are phase singularities in the order parameter field, around which the complex phase of the order parameter changes by $2\pi\kappa$, where $\kappa \in \mathbb{Z}$ is the winding number of the vortex.

In systems described by multicomponent order parameters, the vortex lines may have more complicated structure. A well-known example is the A -phase of ^3He , in which the Cooper paired fermionic atoms possess both orbital and spin angular momentum. The coreless half-integer vortex, for which the phase winding of the order parameter takes half-integer values, was discovered theoretically in such system [2]. Existence of these kinds of topological defects is possible due to the discrete symmetry under combined gauge transformation and spin rotation of the related order parameter. Realization of Bose-Einstein condensates (BECs) in purely optical traps [3] has made it possible to create fractional vortex states also in ultracold atomic gases. In the absence of strong magnetic fields, the hyperfine spin degree of freedom of the atoms is unrestricted, leading to a multicomponent order parameter [4].

Condensates consisting of optically confined spin-2 atoms are of special interest here. The first homotopy group π_1 of the $F = 2$ manifold is non-Abelian [5], enabling non-commutable composition laws for two vortex lines [6]. Topological defects in the so-called cyclic state have been studied theoretically in [7]. The internal symmetry of such order parameter can be mapped to the discrete tetrahedral group, enabling the existence of fractional $1/3$ -vortices. In this paper, we describe two plausible schemes to create controllably a $1/3$ -vortex into the cyclic state of an $F = 2$ spinor BEC. Moreover, we investigate the energetic stability of such states in harmonic

traps under rotation, paving the way towards realization of long-lived non-Abelian topological defects.

An $F = 2$ spinor BEC is characterized by an order parameter which has five spin components, ψ_k , $k = -2, -1, 0, 1, 2$, corresponding to the eigenstates of the five-dimensional representation of the spin operator \hat{S}_z . The different spin populations, $N_k = \int d\mathbf{r} |\psi_k|^2$, can be controlled accurately in an optical trap in the presence of an offset magnetic field [8, 9].

The ground state phase diagram of an $F = 2$ spinor BEC is divided into ferromagnetic, polar, and cyclic regions depending on the values of the spin-spin interaction strength β and the spin-singlet coupling constant γ [10]. This is in close analogy to the phase diagram predicted for d -wave paired Fermi systems [11]. Based on scattering length measurements, the internal ground state of a ^{87}Rb condensate belongs either to the polar or cyclic region [10, 12]. Although several studies have predicted a negative value for γ , implying that the ground state would be polar, due to remaining experimental uncertainties it is not yet clear whether the ground state lies in the cyclic or polar region [13].

By restricting the atom population into the ψ_2 and ψ_{-1} components only, the value of γ becomes insignificant: The spin-singlet pairing interaction does not contribute to the energy since the spin-singlet pairing amplitude, $\Theta = \sum_k (-1)^k \psi_k \psi_{-k}$, vanishes. Hence the internal ground state of such condensate is cyclic. In particular, let us consider states of the form [14]

$$\begin{pmatrix} \psi_{+2}(r, \varphi, z) \\ \psi_{-1}(r, \varphi, z) \end{pmatrix} = e^{i\vartheta} R_z(\phi) \begin{pmatrix} \psi_{+2}(r, z) \\ \psi_{-1}(r, z) \end{pmatrix}, \quad (1)$$

where (r, φ, z) denote the cylindrical coordinates, and ϑ and ϕ are functions of the azimuthal angle φ . $R_z(\phi) = \text{diag}(\exp[2i\phi], \exp[-i\phi])$ describes a spin rotation through an angle ϕ about the z -axis and $e^{i\vartheta}$ is a gauge transformation. By choosing $\vartheta = \phi = \varphi/3$, we obtain a state with unit (zero) phase winding in the ψ_{+2} (ψ_{-1}) component. For such state, by traversing along a loop encircling the origin, the order parameter is continuously transformed onto itself accompanied by

a spin rotation of one-third of a full circle and a phase change of $\frac{2\pi}{3}$. This configuration is therefore called a $\frac{1}{3}$ -vortex state. Similarly, choosing $\vartheta = 2\varphi/3$, $\phi = -\varphi/3$, yields a $\frac{2}{3}$ -vortex state.

Here we restrict to mean-field theory for which the zero-temperature energy of the condensate in the absence of external magnetic fields is given by [10]

$$E = \int d\mathbf{r} \left[\psi_k^* \hat{h}_\Omega \psi_k + \frac{\alpha}{2} n^2 + \frac{\beta}{2} \langle \mathbf{f} \rangle^2 + \frac{\gamma}{2} |\Theta|^2 \right], \quad (2)$$

with implied summation over repeated indices. In Eq. (2), $\hat{h}_\Omega = -\frac{\hbar^2}{2m} \nabla^2 + V_{\text{trap}}(\mathbf{r}) - \mathbf{\Omega} \cdot \hat{\mathbf{L}}$ is the single-particle Hamiltonian where m is the mass of a ^{87}Rb atom, V_{trap} the external optical potential, $\hat{\mathbf{L}}$ the angular momentum operator, and Ω the rotation frequency of the trap. The total density of the condensate is denoted by $n = \psi_k^* \psi_k$, and the spin-spin interaction energy by $\langle \mathbf{f} \rangle^2 = \psi_i^* \psi_k^* f_{ij}^\delta f_{kl}^\delta \psi_j \psi_l$, where f_{kl}^δ is a matrix element of \hat{S}_δ/\hbar . The parameters α , β , and γ are related to the s -wave scattering lengths a_F in the total hyperfine state F according to $\alpha = \frac{1}{7}(4g_2 + 3g_4)$, $\beta = -\frac{1}{7}(g_2 - g_4)$, and $\gamma = \frac{1}{5}(g_0 - g_4) - \frac{2}{7}(g_2 - g_4)$, where $g_F = \frac{4\pi\hbar^2}{m} a_F$ are the bare coupling constants [10, 15].

Minimizing the energy functional, Eq. (2), with a fixed total number of particles, leads to the zero-temperature Gross-Pitaevskii equation for the order parameter

$$\hat{h}_\Omega \psi_k + \alpha n \psi_k + \beta \langle f^\delta \rangle f_{kl}^\delta \psi_l + \gamma \Theta (-1)^k \psi_{-k}^* = \mu \psi_k, \quad (3)$$

where μ is the chemical potential of the system. We have solved Eq. (3), both in pancake and cigar-shaped harmonic traps, in order to find the ground states of the system. In the former case, we choose the axial trapping frequency ω_z large enough so that the condensate dynamics is frozen in the flattened direction, and hence the axial profile of the wave function can be accurately approximated by a Gaussian function. In this limit, the interaction parameter α is replaced by the quasi-2D form $\alpha_{2D} = 2\sqrt{2}\pi\hbar\omega_z a_r [\frac{1}{7}(4a_2 + 3a_4)]$. Setting the radial and axial trapping frequencies to $(\omega_r/2\pi, \omega_z/2\pi) = (100, 1000)$ Hz, respectively, the harmonic oscillator length in the radial direction is $a_r = 1.1 \mu\text{m}$, and we have chosen the value of α_{2D} to correspond to 2×10^4 ^{87}Rb atoms using the scattering length presented in [10]. Moreover, we set $\beta = \alpha/100$, ($\gamma = -\alpha/187$) according to the values measured in [13].

Figure 1 depicts the computed ground state profiles of the condensate for a range of rotation frequencies, Ω , under the constraint that only the $|+2\rangle$ and $|-1\rangle$ components have non-zero population. The top and bottom rows show the density of particles in the $|+2\rangle$ and $|-1\rangle$ components, respectively. The field of view is $20 a_r \times 20 a_r$, and the angular momentum of each component is given inside the figure. The horizontal bar below the figure shows the critical rotation frequencies for which the energies of neighboring ground state configurations

are equal. The ground states are qualitatively similar for different values of Ω within each stability window, and the representative profiles shown refer to the rotation frequency at the middle of the interval. However, the total angular momentum and magnetization $\langle f_z \rangle$ of the condensate varies within each stability window because the population ratio depends on the rotation frequency. For example, for the $\frac{1}{3}$ -vortex state, illustrated in Fig. 1(b), the angular momentum ranges from $0.34 N\hbar$ to $0.40 N\hbar$ and the magnetization from $0.031 N$ to $0.099 N$.

For the chosen parameters, the $\frac{1}{3}$ -vortex state $[\psi_{+2}(r)e^{i\varphi}, \psi_{-1}(r)]$ turns out to be energetically favorable compared to the non-rotating ground state when $\Omega > 0.0957\omega_r$. As the rotation frequency is further increased above $\Omega = 0.123\omega_r$, a pair of $\frac{1}{3}$ - and $\frac{2}{3}$ -vortices occupies the ground state. This state is analogous to the vortex molecule structure discussed in [16] within the nonlinear sigma model. In the present context, the $(\frac{1}{3}, \frac{2}{3})$ -vortex pair can be viewed as a split gauge vortex, because the total spin rotation along a loop containing the pair vanishes and the gauge fields of the individual vortices add up to an integer phase winding $e^{i\varphi}$. The $\frac{2}{3}$ -vortex state carries roughly twice the angular momentum and kinetic energy of the $\frac{1}{3}$ -vortex state. The former becomes energetically favorable compared to the non-rotating ground state at $\Omega = 0.111\omega_r$, and at $\Omega = 0.127\omega_r$ when compared to the $\frac{1}{3}$ -vortex state. However, this state is not the ground state of the system for any value of Ω . For comparison, in the scalar $|F=2, m_F=+2\rangle$ condensate with the same parameter values, the singly quantized vortex state is the ground state within the interval $\Omega \in [0.164\omega_r, 0.222\omega_r]$. We have also confirmed that other possible vortex states in the given configuration, such as gauge or integer spin vortices, are energetically unstable.

At even higher rotation frequencies additional $\frac{1}{3}$ - and $\frac{2}{3}$ -vortices enter the system, yielding a rich structure in the ground state phase diagram, see Figs. 1(d)-(h). With fast enough rotation, lattices consisting of $\frac{1}{3}$ - and $\frac{2}{3}$ -vortices appear. Vortex lattice transitions in such setup have been studied recently [17]. Moreover, vortex lattice structures in two-component condensates have previously been studied theoretically [18, 19], as well as observed experimentally [20]. In the present study, the population ratio is $N_{+2}/N_{-1} \sim 0.5$, instead of being close to unity, which is inherited from the underlying magnetic state (cyclic). For the parameter values of ^{87}Rb , we observe only interlaced square and rectangular vortex lattices. The shape of the unit cell depends on the rotation frequency as well as on the total particle number N , tending more towards a square lattice in the limit $\Omega \rightarrow \omega_r$, and $N \rightarrow \infty$. For example, with $\Omega = 0.90\omega_r$ and $N = 2 \times 10^4$, both unit cells are present: a square lattice close to the trap center where particle density is high, bounded by rectangular unit cells closer to the periphery of the cloud. The magnetization of the interlaced square

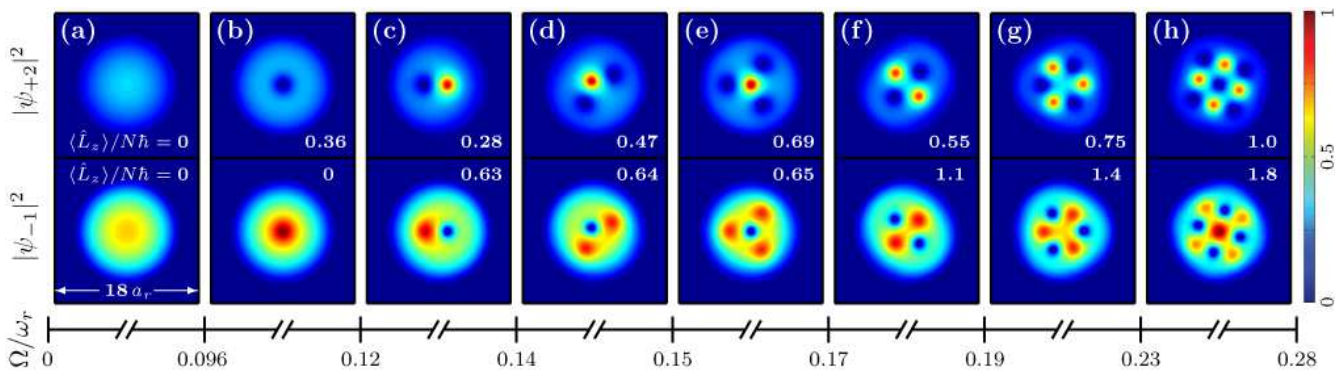


FIG. 1: (Color online) Ground state density profiles of ^{87}Rb atoms in the $|F=2, m_F=+2\rangle$ component (upper row) and $|F=2, m_F=-1\rangle$ component (lower row) in a harmonic trap rotating at frequency Ω under the constraint that only these components are populated. The density minima in the $|+2\rangle$ component correspond to fractional $1/3$ -vortices, and those in $|-1\rangle$ to $2/3$ -vortices. The $1/3$ -vortex is the ground state within the interval $\Omega \in [0.0957 \omega_r, 0.123 \omega_r]$ for the chosen parameter values. The color bar is scaled with respect to the maximum of the total density, $\max[n(\mathbf{r})]$.

lattice resembles notably that of the ground state of a 2D Ising model with antiferromagnetic interactions. Moreover, these vortex lattices can be viewed as consisting of $(1/3, 2/3)$ -vortex pairs, such as depicted in Fig. 1(c).

In the cigar-shaped limit, we choose the trapping frequencies $(\omega_r/2\pi, \omega_z/2\pi) = (100, 10)$ Hz, and the coupling constants $\alpha, \beta, (\gamma)$ corresponding to 3×10^5 ^{87}Rb atoms. The $1/3$ -vortex state is the ground state within the interval $\Omega \in [0.171 \omega_r, 0.237 \omega_r]$. The vortex line is bent in the stationary state of the system even in cylindrically symmetric confinement, analogously to the scalar case [21]. Hence, the angular momentum of the $1/3$ -vortex state is not determined only through the populations in the two components, N_{+2} and N_{-1} , but is strongly affected also by the bending of the vortex line. Within the stability window, the atom number in the $|+2\rangle$ component ranges from $0.33 N$ to $0.41 N$, whereas the total angular momentum ranges from $0.21 N\hbar$ to $0.39 N\hbar$. For comparison, the singly quantized vortex state in the scalar $|F=2, m_F=+2\rangle$ case is energetically favorable within the interval $\Omega \in [0.294 \omega_r, 0.394 \omega_r]$.

As the rotation frequency is increased further, the ground state contains a $(1/3, 2/3)$ -vortex pair which is illustrated in the isosurface plots of Fig. 2 for $\Omega = 0.25 \omega_r$. At each point on the surface shown in Fig. 2(a), the particle density in the $|+2\rangle$ component is equal to 10% of the total particle density, and similarly for the $|-1\rangle$ component in Fig. 2(b). The surfaces are cut open to clarify the vortex lines inside the clouds.

The ground state energy as a function of rotation frequency Ω is plotted in Fig. 2(c) (the solid curve). The interval within which the $1/3$ -vortex is stable is bounded by the dashed vertical lines. The slope of the energy curve steepens as the total angular momentum of the state increases. The angular momentum of each component is shown with circles for $|+2\rangle$ and triangles for $|-1\rangle$. Angular momentum of the $|-1\rangle$ component devi-

ates slightly from zero even in the $1/3$ -vortex state since bending of the vortex line breaks the cylindrical symmetry in both components. For higher rotation frequencies, a square lattice of vortices forms also in the cigar-shaped case.

Finally, we will describe two alternative methods of creating a $1/3$ -vortex state in a trapped condensate. The first scheme is a direct generalization of the method utilized by Matthews *et al.* to create the first vortex in a two-component BEC [22, 23]. The condensate is first prepared in the $|F=1, m_F=0\rangle$ state in an optical trap, e.g., by applying a magnetic field gradient during the evaporative cooling stage [24]. Subsequently, two-photon microwave and auxiliary laser fields are used, as in [23], to transfer roughly one-third of the population directly into a finite orbital angular momentum state in $|F=2, m_F=+2\rangle$. Thereafter, the desired configuration in the $F=2$ manifold is achieved by switching off the laser beam and transferring the remaining population from $|F=1, m_F=0\rangle$ into $|F=2, m_F=-1\rangle$ by a resonant microwave field. The scheme described above yields a $1/3$ -vortex state $[\psi_{+2}(r, z)e^{i\varphi}, \psi_{-1}(r, z)]$ with the desired population ratio of $N_{+2}/N_{-1} \sim 0.5$. Following the same prescription but initially preparing the atoms in $|F=1, m_F=-1\rangle$ results in $[\psi_{+1}(r, z)e^{i\varphi}, \psi_{-2}(r, z)]$ which is a $2/3$ -vortex state. However, in this case some of the initially prepared atoms would have to be discarded in order to obtain the optimal population ratio with maximal transfer of 50% with the two-photon microwave field. The auxiliary far-detuned rotating laser beam could in principle be utilized in rotating the condensate [25], providing stability for the fractional vortex state.

Another possibility to create the $1/3$ -vortex state employs a Laguerre-Gaussian (LG) laser mode which has previously been utilized for creating multiply quantized vortices in a scalar BEC as well as vortex-antivortex su-

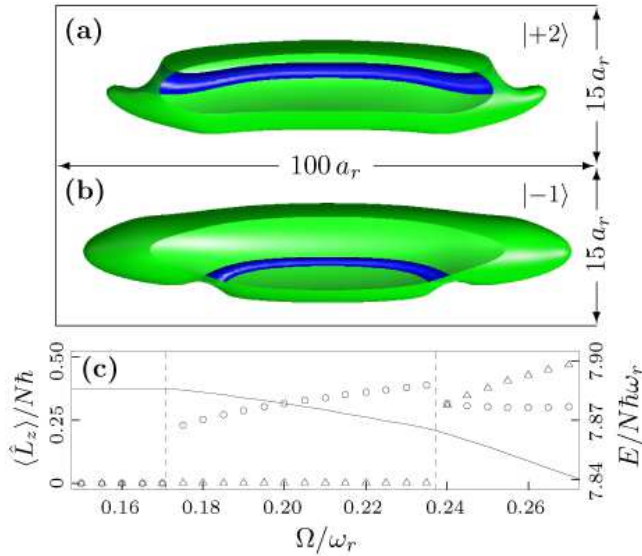


FIG. 2: (Color online) (a) Isosurface plot of the density of particles in the $|+2\rangle$ component $|\psi_{+2}(\mathbf{r})|^2$, and (b) in the $|-1\rangle$ component $|\psi_{-1}(\mathbf{r})|^2$. The field of view is illustrated approximately by the double arrows. In both isosurfaces, the density is equal to 10% of the maximum total density of particles, $\max[n(\mathbf{r})]$. For the chosen rotation frequency of $\Omega = 0.25 \omega_r$, the ground state contains a $(\frac{1}{3}, \frac{2}{3})$ -vortex pair. The vortex lines, for clarity drawn with different color as the rest of the isosurface, are bent even in an axisymmetric trap. (c) Angular momentum in the $|+2\rangle$ component (circles) and in the $|-1\rangle$ component (triangles) as a function of the rotation frequency Ω . The solid curve shows the ground state energy of the condensate. The $\frac{1}{3}$ -vortex is the ground state configuration between the dashed vertical lines.

perposition states in spinor condensates [26, 27]. The $\frac{1}{3}$ -vortex configuration could be achieved by preparing the condensate initially in $|F = 1, m_F = 0\rangle$, and transferring roughly one-third of the atoms into $|F = 2, m_F = +2\rangle$ using counterpropagating σ^+ polarized LG and σ^- polarized Gaussian laser beams [27]. The remaining population in $|F = 1, m_F = 0\rangle$ could be transferred into $|F = 2, m_F = -1\rangle$ using resonant microwave pulses yielding the desired vortex state and population ratio.

In experiments, the lifetime of a condensate in the unstable $F = 2$ manifold has been limited to a few hundred milliseconds due to inelastic collisions [8]. Therefore, it seems more promising to create the $\frac{1}{3}$ -vortex dynamically instead of relying on the cloud to thermalize into the lowest energy state. The magnetization relaxation time scale is beyond current lifetimes of the condensates, and hence the population ratio of the $|+2\rangle$ and $|-1\rangle$ components may be expected to be conserved even in the presence of weak magnetic stray fields. Moreover, very slow spin-mixing dynamics has been reported in ^{87}Rb condensates initially prepared in the cyclic configuration [8], in favor of stable fractional vortex states.

In summary, we have proposed two realistic meth-

ods to create a fractional $\frac{1}{3}$ -vortex state in an $F = 2$ spinor Bose-Einstein condensate in a laboratory experiment. Both schemes are based on transferring population from the stable $F = 1$ manifold into two spin states, $|m_F = +2\rangle$ and $|m_F = -1\rangle$, in the $F = 2$ manifold by using a combination of laser beams and pulsed magnetic fields. We have performed energetic stability analysis of such fractional vortex states, and found that, e.g., the $\frac{1}{3}$ -vortex is the energetically favored state within an interval of rotation frequencies of the confining potential. For increasing rotation frequencies, the ground state contains more and more of $\frac{1}{3}$ - and $\frac{2}{3}$ -vortices, which eventually form an interlaced square lattice. The energetic stability of the fractional vortices under rotation raises hope for experimental realization of topological defects with non-Abelian statistics. Effects related to the non-Abelian nature of the fractional vortices could be probed for instance by vortex-vortex collision experiments [6].

T. Hirano, T. Mizushima and M. Takahashi are acknowledged for useful discussions. The work was financially supported by JSPS and the Väisälä Foundation.

-
- [1] R. J. Donnelly, *Quantized Vortices in Helium II*, (Cambridge University Press, Cambridge, 1991).
 - [2] G. E. Volovik, *Exotic properties of superfluid ^3He* , (World Scientific, Singapore, 1992).
 - [3] D. M. Stamper-Kurn *et al.*, Phys. Rev. Lett. **80**, 2027 (1998).
 - [4] T. Ohmi and K. Machida, J. Phys. Soc. Jpn. **67**, 1822 (1998); T.-L. Ho, Phys. Rev. Lett. **81**, 742 (1998).
 - [5] N. D. Mermin, Rev. Mod. Phys. **51**, 591 (1979).
 - [6] M. Kobayashi *et al.*, Phys. Rev. Lett. **103**, 115301 (2009).
 - [7] H. Mäkelä *et al.*, J. Phys. A **36**, 8555 (2003); H. Mäkelä, J. Phys. A **39**, 7423 (2006); G. W. Semenoff and F. Zhou, Phys. Rev. Lett. **98**, 100401 (2007).
 - [8] H. Schmaljohann *et al.*, Phys. Rev. Lett. **92**, 040402 (2004).
 - [9] T. Kuwamoto *et al.*, Phys. Rev. A **69**, 063604 (2004).
 - [10] C. V. Ciobanu *et al.*, Phys. Rev. A **61**, 033607 (2000).
 - [11] M. D. Mermin, Phys. Rev. A **9**, 868 (1974).
 - [12] N. N. Klausen *et al.*, Phys. Rev. A, **64**, 053602 (2001).
 - [13] A. Widera *et al.*, New J. Phys. **8**, 152 (2006).
 - [14] Without loss of generality, we omit writing the relative phase between the components and restrict the discussion to involve only $|+2\rangle$ and $|-1\rangle$ states whereas all of our results apply also to the $|-2\rangle$ and $|+1\rangle$ combination.
 - [15] M. Koashi and M. Ueda, Phys. Rev. Lett. **84**, 1066 (2000).
 - [16] K. Kasamatsu *et al.*, Phys. Rev. Lett. **93**, 250406 (2004).
 - [17] R. Barnett *et al.*, Phys. Rev. Lett. **100**, 240405 (2008).
 - [18] E. J. Mueller and T.-L. Ho, Phys. Rev. Lett. **88**, 180403 (2002).
 - [19] K. Kasamatsu *et al.*, Phys. Rev. Lett. **91**, 150406 (2003).
 - [20] V. Schweikhard *et al.*, Phys. Rev. Lett. **93**, 210403 (2004).
 - [21] J. J. García-Ripoll and V. M. Pérez-García, Phys. Rev. A **64**, 053611 (2001).

- [22] J. E. Williams and M. J. Holland, *Nature (London)* **40**, 568 (1999).
- [23] M. R. Matthews *et al.*, *Phys. Rev. Lett.* **83**, 2498 (1999).
- [24] M.-S. Chang *et al.*, *Phys. Rev. Lett.* **92**, 140403 (2004).
- [25] K. W. Madison *et al.*, *Phys. Rev. Lett.* **84**, 806 (2000).
- [26] M. F. Andersen *et al.*, *Phys. Rev. Lett.* **97**, 170406 (2006).
- [27] K. C. Wright *et al.*, *Phys. Rev. Lett.* **102**, 030405 (2009).